ELSEVIER

Contents lists available at ScienceDirect

Sensors and Actuators: A. Physical

journal homepage: www.elsevier.com/locate/sna



Maximizing energy efficiency of variable stiffness actuators through an interval-based optimization framework



Trevor Exley^a, Amir Jafari^{a,*}

^a Advanced Robotic Manipulator (ARM) Lab, Department of Biomedical Engineering, University of North Texas, Texas, United States

ARTICLE INFO

Article history:
Received 8 June 2021
Received in revised form 5 September 2021
Accepted 16 September 2021
Available online 25 September 2021

Keywords: Variable stiffness actuators Branch-and-bound Optimization

ABSTRACT

Despite the necessity for being able to regulate the stiffness of the robotic platforms in physical contact with humans, and tremendous number of different variable stiffness actuators that have been developed so far, there is still no such actuator that has successfully passed the research lab phase and transferred into a real application. The main reason is due to the lack of understating on how to optimally design a stiffness adjustment mechanism based on desired performances of each application. If not optimally designed, the additional complexities within the actuators, prevent to win the trade-off between benefits of having a stiffness adjustment mechanisms versus its costs, such as the energy storage capacity of the elastic elements compared to how much energy can be actually released at the output of the actuator, i.e. the link. Currently, this trade-off criterion is not in favor of introducing a stiffness adjustment mechanism into the actuator. Therefor, generally, having a simple series elastic actuator with active compliance has been preferred over having a complex variable stiffness actuator, in many real applications. This work develops an understanding of how to optimally design the parameters of a stiffness adjustment mechanism by developing a framework that can robustly maximize the energy efficiency of variable stiffness actuators. Five different design sets of stiffness adjustment mechanism are being considered and evaluated based on the proposed optimization framework. The resultant optimal design of each set is then compared with the original design in terms of energy efficiency. The proposed framework shows improvement of energy efficiency up to 354%, while design constraints are all being satisfied.

© 2021 Published by Elsevier B.V.

1. Introduction

In the context of physical Human-Robot Interactions (pHRI), the technology required to fabricate the robotic manipulators is fundamentally different than the one developed for traditional industrial robots [7]. The fact that pHRI robots are supposed to physically interact with humans, make industrial robots sources of danger to the soft and delicate body of humans [16]. Furthermore, in contrast to industrial robots that should be operated in isolated work-space from humans where everything about the environment is already known and planned for, the existence of humans in pHRI applications creates highly unknown environments as we, humans, are so unpredictable when it comes to motion, location and interaction forces [4]. In order to guarantee safety of humans in physical interactions with robotic manipulators, actuators as the sources of generating mechanical power should behave soft [17]. There are two

main approaches to make a robotic platform soft; one, that is called active compliance [5,30,31], is through the control framework, where the actuator should be facilitated with force/torque sensors to detect the collision and close loop feedback with different control strategies to prevent or at least reduce the level of risk [6]. This approach, however, cannot guarantee the safety in case of high bandwidth collisions such as impact forces and, as a result, the actuator would behave rigid in such scenarios. The other approach is to realize passive compliance embedded into the mechanical structure of the actuator, so that it can behave inherently soft in any interaction scenario [3,18,38,57,63]. Pioneer in this area, is the Series Elastic Actuator SEA developed by Pratt [41], where a spring was located between the motor and the output link, decoupling the high reflected inertia of the gearbox from that of the link. Therefore, when it comes to an interaction with a human body, only the link inertia will be in contact. Also, the spring can act like a force sensor, allowing to use the active compliance approach to regulate the reflected stiffness through the control framework on top of the mechanical stiffness [42,44]. But again when it comes to high bandwidth interaction

^{*} Corresponding author.

E-mail address: amir.jafari@unt.edu (A. Jafari).

scenarios, the stiffness of a SEA would be the fixed stiffness level of its embedded spring [21].

Also note that, spring can save and release the energy, which in periodic motions can greatly enhance the energy efficiency [39,49]. However, in case of a SEA, this would be beneficial only when the frequency of the desired periodic motion matches the natural frequency of the compliant actuator [59]. In order to exploit the full advantage of having a source of storing and releasing energy, i.e. spring, in periodic motions with different frequencies, the mechanical stiffness level of the actuator should be adjustable [25,58]. Furthermore, In general, when a robotic manipulator moves fast, it should be soft to guarantee safety and when it moves slow and accuracy is desired, it should be rigid [52].

Variable Stiffness Actuators (VSAs) [24,46,61,64], have been developed to address these needs in pHRI applications. A VSA needs two motors as it has to control two degrees of freedom; one is the output link's position just like a normal rigid actuator and the other one is the output link's stiffness [23,26,28]. Regulating the stiffness in VSAs is done by different Stiffness Adjustment Mechanisms (SAMs) that contain springs and other components [22]. SAMs can be categorized into two design groups; *Antagonistic* and *Series* [27]. In antagonistic designs, both motors are responsible to control the output link position and regulating its stiffness, whereas in series designs, one motor is dedicated to the link positioning while the other one adjusts the stiffness.

Despite the great need of being able to regulate the stiffness of the robotic actuators in pHRI applications and tremendous number of different VSAs that have been developed so far, to our knowledge, there is not a VSA that has successfully passed the research lab phase and transitioned into a real application. The main reason is due to the lack of understating how to optimally design a SAM based on desired performances of different applications.

In [29] some determinants for stiffness adjustment mechanisms were introduced and performance of different mechanisms were analyzed against the determinants. The mentioned work explained these determinants and presented a comprehensive framework to systematically analyze performances of different stiffness adjustment mechanisms. First, a classification of different stiffness adjustment mechanisms was presented. Then, characteristics of each class regarding different determinants were evaluated and compared through numerical analysis. However, so far, no research work has addressed the optimal design problems with VSAs.

Another work analyzed the correlation between the external loads, applied to different variable stiffness actuators, and their resultant output stiffness. Different types of variable stiffness actuators were studied considering springs with different types of nonlinearity [22]. In addition, in [27] different variable stiffness design approaches with different types of springs (linear, quadratic, exponential and cubic) are analyzed and compared with respect to the energy required to regulate the stiffness. The results gave some insights about the design parameters which mostly affect the energy consumption for the stiffness adjustment. However, these previous research works have not addressed the problem of optimal design parameters.

If not optimally designed, the additional complexities that SAMs present to the actuators prevent to win the trade-off between benefits of having a SAM versus its costs. Some examples of these trade-off criteria are as following: the energy saving benefit of adjusting the stiffness in different periodic motions compared to how much energy is in fact required for the stiffness regulation, increased toque capacity due to having two motors compared to how much torque can be actually transferred to the output link, energy storage capacity of the springs compared to how much energy can be actually released at the output link side, and adjusting the stiffness to a certain value compared to what is the actual stiffness of the output link in dealing with unknown external forces. Currently, these trade-

off criteria are not in favor of introducing a SAM into the actuator. Therefor, generally, having a simple series elastic actuator with active compliance has been preferred over having a complex VSA [12,13]. This research seeks to understand how to optimally design the parameters of a SAM by developing a framework that can robustly maximize the energy efficiency of VSAs for pHRI applications.

Depends on a particular design, the design parameters of a SAM may include the dimensions of its principal components, e.g. cam, level arm, pulleys, etc, and stiffness of its springs. The constraints are user defined torque and velocity limitations of the motors, springs' constants (stiffnesses), and size limitations of the principal components.

The dimensions of principal components are real continuous variables, while stiffness of the spring and their dimensions, e.g. diameter, length and maximum allowable deflections, are categorical variables as springs are commercial products that come in different but discrete sizes and stiffness constants. The same holds true for motors and theirs maximum torques and velocities. Furthermore, since power is a product of torque and velocity, the nature of any energy-based optimization problem would be nonlinear. Therefore, we will be dealing a mixed-integer nonlinear optimization problem with large number of feasible solutions [9]. To solve this type of optimization problem, there are basically two main approaches; Heuristic (or Meta-Heuristic) [33] and Global optimal [20]. The heuristic approaches can quickly find optimal solutions but cannot guarantee that the yield solutions are the global optimum (as they may get trapped into local optimal solutions). Examples are: Tabue search [11], Simulated annealing [54], and Ant colony optimization [8]. The global optimal approaches, on the other side, may take a long time to find a solution, but once it is found, the solution is guaranteed to be the global optimal. Since computation time is not a critical factor in optimal design problems, therefore global optimal approach is preferred over the heuristic one. Examples are: Cutting plane method [15], Branch and Bound (BB) algorithm [32] and Interval method [19].

For this optimal design problem, we propose to employ interval method as a mean to systematically enumerate candidate solutions in a BB algorithm. The so called interval based branch and bound algorithm can deal with nonlinear mixed-integer problems and has been shown to be effective in optimal actuator design problems, in particular [35,36].

This article is organized as follow: in Section 2, different sets of stiffness adjustment mechanism are introduced and their principal dimensions will be extracted. Section 3, explains the proposed optimization framework, while Section 4 elaborates on the results obtained from the optimization framework and compares them with the original designs. Finally Section 5 presents conclusion and future works.

2. Stiffness adjustment mechanisms - design sets and principal dimensions

VSAs have been developed to address the safety, limited adaptability in interaction with uncertainties and energy efficiency issues which exist in traditional "stiff" robots. These types of actuators have two motors to regulate the stiffness and the position of the attached link. Springs are embedded into the system to realize the variable stiffness functionality using different design principles. In general, these designs can be divided into two main classes: antagonistic and series [55,56].

In antagonistic designs, two motors M_1 and M_2 are antagonistically actuating a link through nonlinear springs (i.e. nonlinear force to deflection profile) that are placed between the motors and the link. The nonlinearity of the springs is an important factor as stiffness regulation cannot be achieved using linear springs in these setups. Based on different arrangements of the motors and springs,

Antagonistic Class

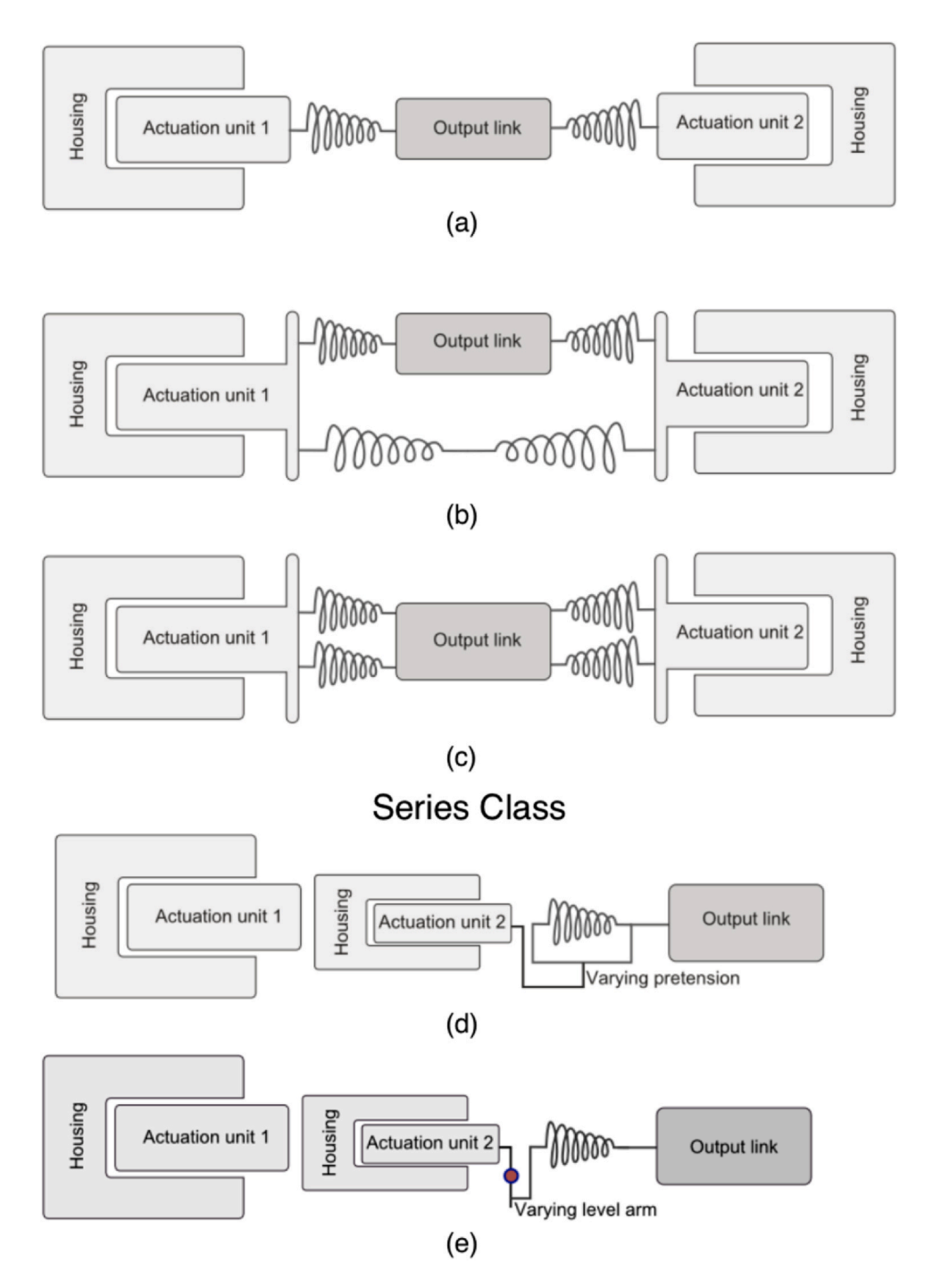


Fig. 1. Different classes of SAMs: Antagonistic Class: a) simple antagonistic, b) cross-coupling, c) bi-directional- Series Class: d) pre-tension based, and e) lever-based.

these types of designs can be realized in three different sub-classes: simple unidirectional (e.g. [34]), cross coupling (e.g. [46]) and bi-directional (e.g. [40]) configurations as it is shown in Fig. 1-a-b-c.

Alternatively, in the series design approaches, one motor M_1 with a spring in series is dedicated to the link positioning while another motor M_2 (usually smaller than M_1) is set to change the stiffness. In one class of these design approaches (Fig. 1-d), nonlinear springs are employed where stiffness adjustment is done through changing the pre-tension of the springs using M_2 . Another class of these design approaches (lever-based) (Fig. 1-e) uses linear springs while the

stiffness adjustment is done through changing another parameter such as location of the springs [26], the pivot point [24,50,51,53] or the point at which force is being applied to a lever mechanism [14].

These design approaches can be realized in many different ways, using different mechanisms or components. However, regardless of how they have been realized, there are always principal components in each class whose dimensions or properties are essential in determining functionality of the SAM as well as output performance of the VSA. In antagonistic SAMs, examples are: the radius of the link's

pulley, the radius of each motor's pulley, the distances between center of rotation of each pulley as well as springs' constants.

In those SAMs that need nonlinear springs, sometimes linear springs are used together with a mechanism that can generate nonlinear force to deflection profile, such as cam-follower mechanism in contact with a spring [45]. In this case, dimension of cam is also another principal component of the SAM as its profile determines the nonlinearity of the spring.

In our proposed optimal design process, we only take into account the principal components of a SAM, rather than every single elements (such as bearings, screws, etc) that are being used in a particular realization. However, our proposed approach is general and one can consider different detailing levels of a particular SAM in the optimization process. However, it may substantially add to the complexity of the process by increasing the number of variables while the output optimal result might not be significantly better.

In addition, each motor M_1 and M_2 provides energy to the SAM that can be presented by considering torques and displacement/velocity of an element due to that torque (e.g. motor shaft). Motors come in different torque and velocity capacities. These parameters which eventually affect the output performance of a VSA are discrete categorical variables. The same holds true for springs as they have different spring constants, sizes, free length, and maximum allowable deflections, which all can affect the performance of a VSA.

Therefore, in order to optimize the design process, different types of variables including continuous and integer or categorical variables have to be dealt with. This makes the design problem a nonlinear mixed-integer optimization problem.

3. Optimization framework

As discussed before, to design a SAM, we are dealing with some continuous design variables such as dimensions of its principal elements as well as some categorical variables such as stiffness, free length, diameter and maximum allowable deflection of the springs. We present continuous variables as vector $P_r \in IR^n$ (where n is the number of continuous variables) and categorical variables as $P_c \in \prod_{i=1}^{c_n} K_i$ (where c_n is the number of categorical variables).

This research work focuses on how to optimally design a SAM in order to maximize energy efficiency of a VSA when the output link capacity with regards to its energy saving storage is given. The reason this aim is important is the fact that SAMs are basically energy storage and release elements of VSAs. They are located between the source of the energy to the system, i.e. motors M_1 and M_2 and the output link where energy is being transmitted to the external environment. By maximizing energy storage and release ratio, we actually minimize the amount of energy that is stored in a SAM but cannot actually be delivered at the output link.

3.1. Cost function formulation

Energy storage capacity of a SAM depends on number of springs as well as stiffness and maximum allowable deflection of each spring. All these parameters affect the overall size and weight of the SAM and eventually those of a VSA. The maximum energy storage capacity of a SAM E_{SAMmax} can be expressed as follow:

$$E_{SAM_{max}} = \sum_{i=1}^{n_s} \int_0^{\delta_{smax_i}} \int_0^{\delta_{smax_i}} K_{s_i} d\delta_s d\delta_s$$
 (1)

where, $\delta_{s_{max_i}}$ and K_{s_i} are maximum allowable deflection and stiffness of *i*th spring, respectively, while n_s is the total number of springs in a SAM. All these design parameters are categorical variables.

On the other side, the output performance of a VSA depends on how much elastic energy can be stored into its output link. The maximum energy that can be stored at the output link is:

$$E_{L_{max}} = \int_0^{\delta_{L_m ax}} \int_0^{\delta_{L_m ax}} K_L d\delta_{L_m ax} d\delta_{L_m ax}$$
 (2)

where K_L and δ_{L_max} are the output link's stiffness and maximum deflection, respectively. These two design parameters are functions of both real continuous and categorical variables.

If some part of energy storage capacity of the SAM cannot be released to the output link, it is actually wasted from the output link's perspective, while it takes space (and also adds unnecessary weight to the overall system) to store that wasted part of energy inside the SAM. In a perfect scenario, the whole amount of energy that is stored into a SAM, should be released and be available to the output link, i.e. $E_{SAM_{max}} = E_{L_{max}}$. In order to make VSAs lighter, more compact but yet more functional, the ratio between the energy storage capacity of the SAM and the energy released to the output link $f(P_c, P_r) = E_{SAM_{max}} / E_{L_{max}} \ge 1$ should be minimized.

Therefore, the optimization problem can be expressed as:

$$\begin{cases} P_{c} \in \mathbb{R}^{n}, P_{c} \in \prod_{i=1}^{c_{n}} K_{i} f(P_{c}, P_{r}) \\ \text{subject to:} \\ g_{i}(P_{c}, P_{r}) \leq 0, \ \forall \ i \in 1, ..., l \\ h_{j}(P_{c}, P_{r}) = 0, \ \forall \ j \in 1, ..., m \end{cases}$$
(3)

where $g_i(P_c, P_r)$ and $h_j(P_c, P_r)$ are constraints that will be discussed in the following subsection.

We will formulated this optimization problem 3 for each 5 classes of SAM designs. This mixed-integer optimization problem is in fact an inverse design problem as oppose to a direct design problem. However, problems of this type are generally nonlinear, non-quadratic, and also nonconvex. Generally, for these problems, the knowledge of all the expressions of the functions of the considered problem can be found through the principal components and their interactions based on what class of VSAs designs the SAM belongs to. However, the solution could not be found by iterating some resolution of the direct problem as there are large number of feasible solutions.

3.2. Constraints formulation

The constraints of this optimization problem are due to the limitations on real continuous design variables, torque and velocity of the motors M_1 and M_2 as well as springs' maximum allowable deflections $\delta_{s_{max}}$. Here we just presents some examples for each type of these constraints.

-Design constraints: In antagonistic designs, the principal components are basically the pulleys attached to each motor's shaft and the output link, as well as the connections between each pair of pulleys (that can always be modeled as series combinations of rigid and extendable, i.e. springs, elements). The dimensions of interest therefore, are each pulley's radius r_{M_1} , r_{M_2} , r_p as well as the distance between each pair of pulleys d_1 , d_2 , d_3 . The distance between each pair of pulleys can be determined by taking into account the free length and maximum allowable deflection of the spring that should be placed between the two pulleys. For instance, for simple antagonistic class as shown in Fig. 1-a, this means that: $l_{0_1} + \delta_{s_{max_1}} \le d_1$.

In addition to that, there is another important design consideration for antagonistic VSAs: in order to achieve symmetrical behavior as well as contribution of both motors in moving the output link, springs have to be placed with a pre-tension and that pre-tension has to be half of their maximum allowable deflection, so when one spring becomes fully deflected, the other one will reach its free length. This pre-tension will also affect the maximum output link's deflection $\delta_{L_{max}}$. For instance for the spring #1 in the antagonistic class as shown Fig. 1-b, this means that: $r_P \times \delta_{L_{max}} \le 0.5\delta_{s_{max}}$.

In series, pre-tension based class, design variables that can define the profile of the cam are essential. It is important to mention here that the cam is a representative component of this class and it does not mean that all the pre-tension based VSA use a cam mechanism. However, SAM functionality of every pre-tension based VSA can be modeled using a cam profile. It is important to define the cam profile as a function of output link's deflection, i.e. $r_c = f(\delta_L)$. Another design variable in this class that can define the range of stiffness adjustment is the distance between the output of the stiffness motor and the center of rotation of the output link as shown in Fig. 1-d, d_c . This distance should allow for full deflection of the spring at no-load condition: $l_0 + r_{c_{at\delta_L} = 0} + \delta_{s_{max}} \le d_c$.

In series class based on lever mechanism, length of the lever d_l is an important variable to achieve a desired range for stiffness. Also in both series classes, i.e. the pre-tension based and the lever based, a transmission system TS (e.g. a ball screw mechanism) is required to convert rotary motion of the stiffness motor M_2 into a linear motion. The conversion factor can be denoted by variable set N_{TS} that includes all variables that are required to define the torque/force and rotary/linear motion relationships.

-Actuator constraints: In majority of the current VSAs, motors M_1 and M_2 are usually electric DC motors. In these motors, the available torque is limited by the Stall torques T_{s_1} and T_{s_1} and the maximum velocity is ω_{max_1} and ω_{max_2} : $\dot{\theta}_{M_i} \leq \omega_{max_i}$ and $T_{M_i} \leq T_{s_i} \ \forall \ i \in 1, 2$.

Furthermore, in these types of electric DC motors the available torque is a function of velocity: which is the faster the motor runs the less torque it can apply: $T_{M_i} = T_{s_i} \times \left(1 + \theta_{M_i} / \omega_{max_i}\right) \forall i \in 1, 2$.

It is important to mention that motor M_1 and M_2 are commercially available products and thus T_{M_1} , T_{M_2} , ω_{max_1} and ω_{max_2} are related to categorical variables as they come in different discrete values, depending on their types, sizes and manufacturers.

-Spring constraints: Springs are also commercially available products that come in different types and sizes and thus their stiffnesses (spring's constants) k_s , free lengths l_o , and maximum allowable deflections $\delta_{s_{max}}$ are categorical variables. Actual length of the spring at any time cannot be less/more that its free length when the spring is extension/compression type and also their amount of deflection at any time should be less than or equal to their maximum allowable deflection. In case of extension springs, for example: $l_s \geq l_o$ and $\delta_s \leq \delta_{s_{max}}$.

It is also important to highlight here that commercially available springs are either extension or compression type, and therefore, in our models we don't assume a spring that can be both extended or compressed.

Another important feature of the springs that can be considered here is related to their free length. Sometimes springs have some level of pre-tension already built in their structure. This means that there is a threshold force level that needs to be overcome in order for the spring to start deflecting. This amount of force threshold affect the effective free length of the spring that is different that its actual free length. The actual free length is the length of the spring when there is no force acting on it, while the effective free length is by taking into account how much the force threshold could deflect the spring in the opposite direction and then subtract that amount from the actual free length of the spring.

3.3. Interval based BB algorithm

In order to find the global optimal solution to the problem 3, we propose to use interval based BB algorithm, as it is guaranteed that the global solution will be precisely enclosed at the end of the algorithm.

The principle of this algorithms is based on subdivisions of the considered initial domain into smaller and smaller parts such that one can determine, using interval analysis [37], which box can be discarded. This is because interval computations will produce the proof that a box cannot contain the global solution or prove the fact that at least one constraint could not be satisfied in a box. Therefore,

at the end of the algorithm, the global optimum will be enclosed with a given accuracy, however the algorithms must be capable to deal with both real continuous and categorical variables.

The main idea is to subdivide the initial domain space $X \subseteq R^n \times \prod_{i=1}^{c_n} K_i$ into smaller sub-boxes $Z \subseteq X$ and to delete the considered box Z, if and only if it can be proven that Z cannot contain the global optimum.

In order to subdivide the domain into smaller boxes, we need to consider the space in which the boxes are located in. In this problem, this space is a combination of continuous as well as categorical variables.

BB algorithms have been modified to deal with integer variables, such as in the author's previous work in finding an optimal solution to the facility layout problem [47]. The categorical variables cannot be directly considered in subdivision of a box and an expression of a function. In this project, we propose a method to change categorical variables into integer ones. This is done through an univariate function a that assigns an integer to a categorical value. For example, if one spring has stiffness of 315 N/mm and stiffness of another spring is $450.5 \, \text{N/mm}$, this univariate function assigns integer value = 1 to the first stiffness value and integer value = 2 to the second one: $a(1) = 315 \, \text{N/mm}$ and $a(2) = 450.5 \, \text{N/mm}$. Therefore, while integer values 1 and 2 can be used for the purpose of subdividing the boxes, the values a(1) and a(2) will be used in calculating the objective function and constraints.

The classical principle of subdividing is to choose a coordinate direction parallel to which Z has an edge of maximum length. Then, Z is subdivided normal to this direction [37]. For continuous variables the subdivision of a box Z on its kth component into to boxes Z_{1k} and Z_{2k} will be applied at the midpoint (as defined in [37]) of the original box Z as follow: $Z_{1k} = [Z_k^L, (Z_k^U + Z_k^L)/2]$ and $Z_{2k} = [(Z_k^U + Z_k^L)/2], Z_k^U]$, where Z_k^L and Z_k^U denote the lower and upper bounds of kth component of box Z, respectively. For categorical variables, however, this subdivision rule has to be slightly modified as follow: $Z_{1k} = [Z_k^L, [(Z_k^U + Z_k^L)/2]_I]$ and $Z_{2k} = [[(Z_k^U + Z_k^L)/2]_I + 1, Z_k^U]$, where $[x]_I$ is the integer part of x.

At each step of the BB algorithm, and as the branches are generated through subdividing the boxes, we will have an interval for each variable. The interval analysis proposed by [37] is a powerful tool to calculate upper and lower bounds of a function over a box. This is simply done by the concept of *natural extension* of a function.

The natural extension of an expression of f into interval consists by replacing each occurrence of a variable by its corresponding interval (which encloses it), and then by applying the rules of interval arithmetic as explained in [37]. For example, if $f(x) = x^2 + x + 1$ and $x \in X = [1,2]$, then $F(X) = ([1,2])^2 + [1,2] + 1$ (X and F(X) are both intervals) is the natural extension of f(x) over box X. It has been proven by [43] that the natural extension is always an inclusion function, which means that it encloses the upper and lower bounds of f over the box (or even all boxes when dealing with multiple variables) X. Therefore, $f(X) = [\min f(x), \max f(x)] \subseteq F(X) \ \forall X$.

Interval arithmetic is only defined for continuous functions, and thus in our method, the inclusion functions must be extended to deal with discrete variables as well. As mentioned before, we will convert categorical variables into integer variables through univariate functions. These integer variables will then be further relaxed into continuous variables. For example, if an integer variable belongs to set Z^L , $Z^L + 1$, $Z^L + 2$, . . . , Z^U , a continuous interval $[Z^L, Z^U]$ will be considered for this variable. Replacing an integer set by its corresponding relaxed continuous interval, an inclusion function can then be constructed. The proof is obvious because it comes from the fact that the relaxed compact interval sets enclose by definition the initial discrete sets.

In order to proceed with the elimination of the boxes that cannot contain the global optimum solution, just the computation of lower

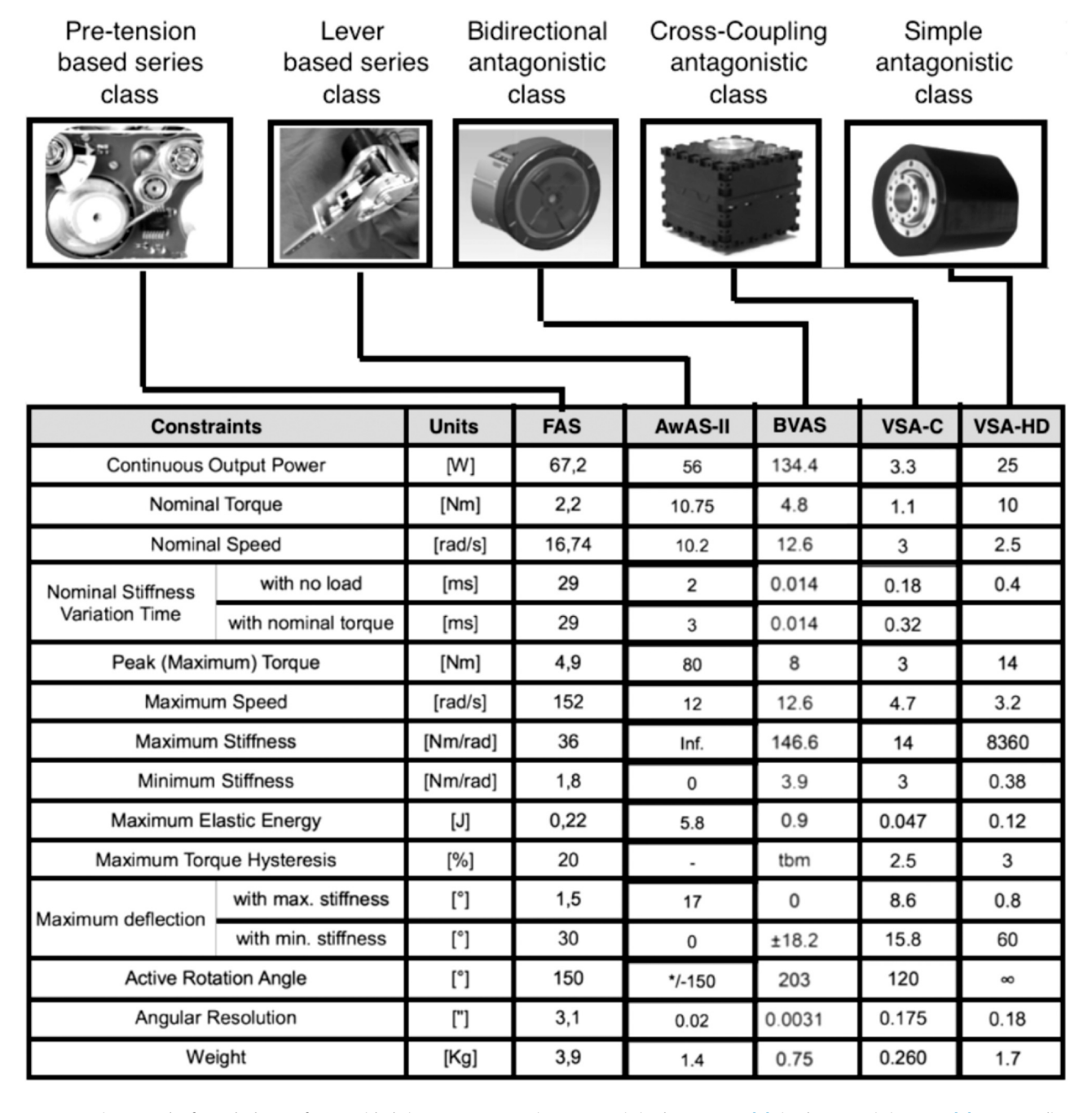


Fig. 2. Representative examples for each classes of SAMs with their actuators' constraints: Antagonistic Class: VSA-HD [1] simple antagonistic; VSA-C [2] cross-coupling; BVAS [40] bi-directional- Series Class: FSA [10] pre-tension based, and AwAS-II [24] lever-based. All data extracted from VIACTORS project's website: https://viactors.org.

bound of a given function f over a box Z, i.e. lb(f,Z), is needed. We will compute these bounds by using interval analysis as follow: Considering that \tilde{f} denotes the current solution (in fact, it is just the best evaluation of f at this stage of the algorithm such that all the constraints are satisfied), one obtains the following:

1) No global solution is in Z, if $ib(f,Z) > \tilde{f}$, a lower bound of f over Z is greater than a solution already found, then no point in Z can be a global minimum.

2) No feasible solution is in Z, if it exists k such that $ib(g_k, Z) > 0$, or it exists k such that $ib(h_k, Z) > 0$ or $ub(h_k, Z) > 0$ (ub=upper bound). In this case, a very small positive real value can be considered instead of 0, in order to address numerical approximation difficulties due to the floating point operations [37].

This implies that at the end of the algorithm, accurate enclosures of the global minimum value and of all their corresponding solutions

can be expected. Indeed, at each step of the algorithm, one has the following properties for all the remaining sub-boxes $Z \subseteq X$: 1) $lb(f, Z) \le \tilde{f}$ and 2) all constraints are always satisfied.

4. Results and discussion

Five Representative examples of SAMs classes, Fig. 2, with their actuators' constraints are being considered as following: Antagonistic Class: VSA-HD [1] simple antagonistic; VSA-C [2] cross-coupling; BVAS [40] bi-directional- Series Class: FSA [10] pre-tension based, and AwAS-II[24] lever-based. Data regarding both actuators and designs constraints for each actuator is extracted from Variable Impedance ACTuation systems embodying advanced interaction behaviORS (VIACTORS) project's website [62]. There are two missing values, first one is regarding the maximum torque hysteresis of

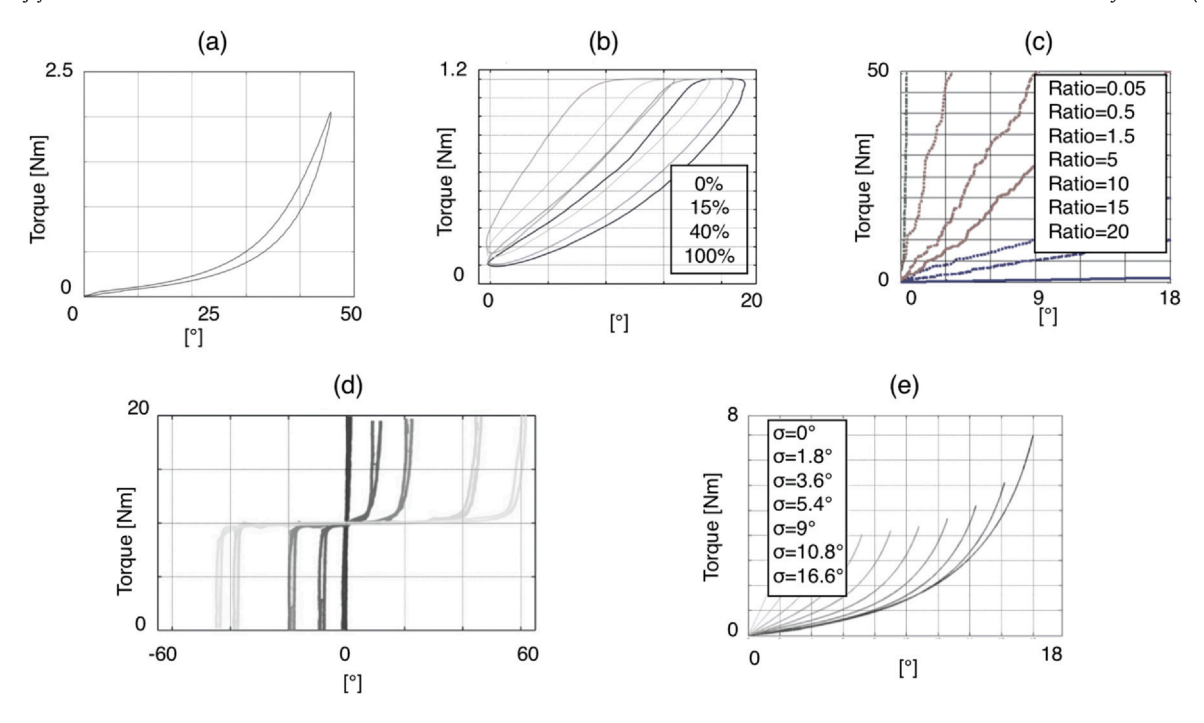


Fig. 3. Plotting static stiffness by applying a known torque and measuring the link deflection for: a) FSA [10], b) VSA-C [2], c) AwAS-II [24], d) VSA-HD [1] and e)BVAS [40]. Stiffness is the slop of each curve.

AwAS-II, which is being adopted from its previous version AwAS [26] as 21%, and the second one is the nominal stiffness variation in time for VSA-HD with nominal torque, which is being considered to be 0.4 ms as the nominal stiffness variation in time with no load.

The energy equation for each of these five representative actuator example has been provided in VIACTORS's data sheets on the specification page, row number 102 [62]. These energy equation are functions of joint stiffness, link deflection and other principal dimensions for each actuator. Plugging the provided energy functions into Eqs. 1, 2 and performing the proposed optimization procedure on each actuator, the optimal design parameters for each actuator can be achieved while the design's and actuator's constraints presented in Fig. 2 are all being satisfied.

For each actuator, the torque versus link deflection, Fig. 3 has been obtained experimentally by applying a known weight to the tip of the link at a known distance (hence a known torque) and measuring the resultant angular deflection through a link encoder, while stiffness has been set to different levels in an off-line fashion. The static stiffness can then be calculated by taking derivative of each resultant torque versus deflection curve, to validate the stiffness regulation formulas that have been provided in the actuator's data sheet in [62]. The calculated stiffness values are actuators' constraints that have to be satisfied while searching for optimal design parameters using the proposed algorithm.

The result of the interval-based optimization framework is presented in Figs. 4 and 5 for all five representative actuators.

In Fig. 4,the maximum energy stored at the link of each actuator in its original design is plotted against that value when the actuator is optimally designed. The plotted value for the original actuators are in fact among the constraints mentioned in Fig. 2, and thus the optimization framework is forced to maintain those levels. However, as it is clear from the figure, some slight deviations have been noticed, even on the negative side. This is due to the floating-points round-off errors that are inevitable when dealing with mixed-integer optimization problems [48].

Fig. 5 shows the maximum energy storage for each representative actuator example for its original as well as optimal designs. As it is clear from this figure, the maximum energy storage

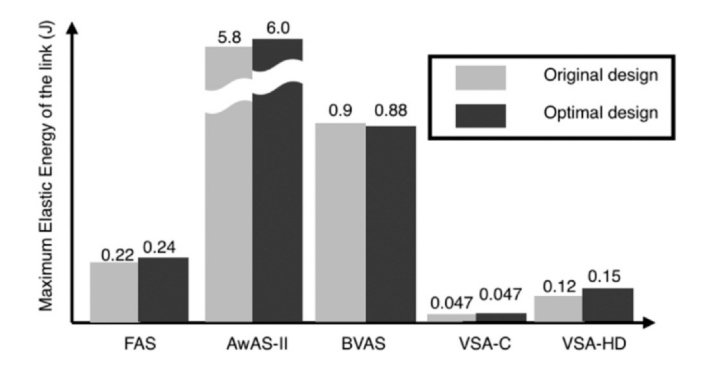


Fig. 4. Maximum elastic energy of the link for FSA [10], AwAS-II [24], BVAS [40], VSA-C [2], VSA-HD [1], with original and optimal designs.

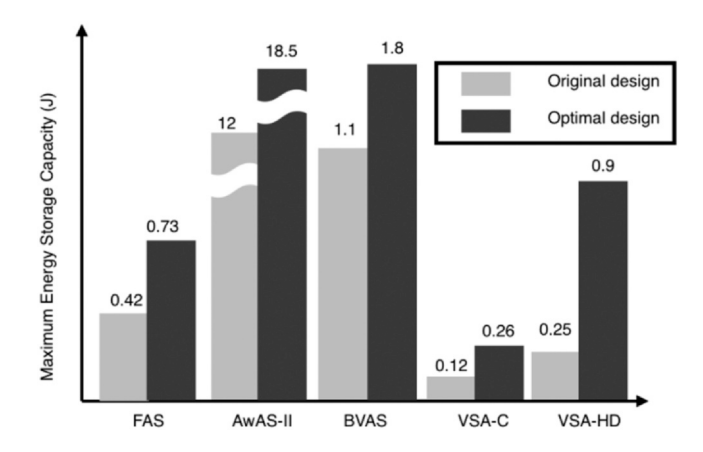


Fig. 5. Maximum energy storage capacity for FSA [10], AwAS-II [24], BVAS [40], VSA-C [2], VSA-HD [1], with original and optimal designs.

of all five actuators improved as the result of optimization algorithm, which the highest improvement belongs to VSA-HD actuator of around 260%.

The energy efficiency of each actuator is in fact, the maximum energy storage capacity of the actuator over the maximum elastic energy of its link, according to Eq. 3. The energy efficiency for all five actuators shows improvement as following: FSA by 154%, AwAS-II by 136%, BVAS by 160%, VSA-C by 212% and VSA-HD by 354%.

5. Conclusion

This paper presents an interval-based optimization framework to maximize the energy efficiency of variable stiffness actuators, which is defined as the maximum energy that can be stored inside elastic elements of an actuator over the maximum elastic energy that is available to the output link. Maximizing energy efficiency of a variable stiffness actuator is an important aspects of the design as this type of actuator has the capability of storing and releasing energy which can help to minimize energy consumption while performing periodic motion [60,61]. Different design parameters are involved in such optimization including continuous, integer and even categorical variables. The proposed algorithm can deal with mixed-integer variables with a technique to convert categorical variables into integer ones. Five different variable stiffness actuators have been taken into account, each represents a class of stiffness adjustment mechanisms, namely: simple antagonistic- cross-coupling, bidirectional, pre-tension based series and lever based series classes.

The results of the optimization framework showed improvements in energy efficiency of all five representative actuators, as high as 354%. Such huge improvements implies the need to optimally designing variable stiffness actuators for specific applications in order to maximize their fusion into the real industrial markets.

Future work aims to consider another cost functions such as robustness or output performance depending on the requirement of different applications, in terms of, for example, link trajectories or torque/stiffness profiles.

Declaration of Competing Interest

The authors declare that they have no known competing financial interests or personal relationships that could have appeared to influence the work reported in this paper.

Acknowledgements

This work has been partially supported by the Nationala Science Foundation (NSF) award number 2045177.

References

- M.G. Catalano, G. Grioli, F. Bonomo, R. Schiavi, A. Bicchi, Vsa-hd: From the enumeration analysis to the prototypical implementation, 2010 IEEE/RSJ Int. Conf. Intell. Robots Syst. (2010) 3676–3681 (IEEE).
- [2] M.G. Catalano, G. Grioli, M. Garabini, F. Bonomo, M. Mancini, N. Tsagarakis, A. Bicchi, Vsa-cubebot: a modular variable stiffness platform for multiple degrees of freedom robots, 2011 IEEE Int. Conf. Robot. Autom. (2011) 5090–5095 (IEEE).
- [3] D. Chakarov, Study of the passive compliance of parallel manipulators, Mech. Mach. Theory 34 (3) (1999) 373–389.
- [4] A. Cherubini, R. Passama, A. Crosnier, A. Lasnier, P. Fraisse, Collaborative manufacturing with physical human-robot interaction, Robot. Comput. -Integr. Manuf. 40 (2016) 1–13.
- [5] Davies, B., Harris, S., Lin, W., Hibberd, R., Middleton, R., Cobb, J. Active compliance in robotic surgery-Ťthe use of force control as a dynamic constraint. Proceedings of the Institution of Mechanical Engineers, Part H: Journal of Engineering in Medicine 211 (4), 285–292, 1997.
- [6] A. De Luca, F. Flacco, Integrated control for phri: Collision avoidance, detection, reaction and collaboration, 2012 4th IEEE RAS EMBS Int. Conf. Biomed. Robot. Biomechatronics (BioRob) (2012) 288–295 (IEEE).
 [7] A. De Santis, B. Siciliano, A. De Luca, A. Bicchi, An atlas of physical human-robot
- [7] A. De Santis, B. Siciliano, A. De Luca, A. Bicchi, An atlas of physical human-robo interaction, Mech. Mach. Theory 43 (3) (2008) 253–270.
- [8] Dorigo, M., DiCaro, G., 1999. Ant colony optimization: a new meta-heuristic. In: Proceedings of the 1999 congress on evolutionary computation-CEC99 (Cat.No. 99TH8406). 2. IEEE, 1470–1477.

- [9] C.A. Floudas, Nonlinear and Mixed-integer Optimization: Fundamentals and Applications, Oxford University Press, 1995.
- [10] W. Friedl, M. Chalon, J. Reinecke, M. Grebenstein, et al., Fas a flexible antagonistic spring element for a high performance over, 2011 IEEE/RSJ Int. Conf. Intell. Robots Syst. (2011) 1366–1372 (IEEE).
- [11] F. Glover, M. Laguna, Tabu search, Handbook of Combinatorial Optimization, Springer, 1998, pp. 2093–2229.
- [12] M. Grimmer, M. Eslamy, S. Gliech, A. Seyfarth, A comparison of parallel-and series elastic elements in an actuator for mimicking human ankle joint in walking and running, 2012 IEEE Int. Conf. Robot. Autom. (2012) 2463–2470 (IEEE).
- [13] M. Grimmer, A. Seyfarth, Stiffness adjustment of a series elastic actuator in an ankle-foot prosthesis for walking and running: the trade-off between energy and peak power optimization, 2011 IEEE Int. Conf. Robot. Autom. (2011) 1439–1444 (IEEE)
- [14] S.S. Groothuis, G. Rusticelli, A. Zucchelli, S. Stramigioli, R. Carloni, The variable stiffness actuator vsaut-ii: mechanical design, modeling, and identification, IEEE/ ASME Trans. Mechatron. 19 (2) (2013) 589–597.
- [15] M. Grötschel, Y. Wakabayashi, A cutting plane algorithm for a clustering problem, Math. Program. 45 (1–3) (1989) 59–96.
- [16] S. Haddadin, A. Albu-Schäffer, G. Hirzinger, Safety evaluation of physical humanrobot interaction via crash-testing, Robot.: Sci. Syst. 3 (2007) 217–224.
- [17] S. Haddadin, E. Croft, Physical human-robot interaction, Springer Handbook of Robotics, Springer, 2016, pp. 1835–1874.
- [18] R.v. Ham, T. Sugar, B. Vanderborght, K. Hollander, D. Lefeber, Compliant actuator designs, IEEE Robot. Autom. Mag. 3 (16) (2009) 81–94.
- [19] E.R. Hansen, Global optimization using interval analysis: the one-dimensional case, J. Optim. Theory Appl. 29 (3) (1979) 331–344.
- [20] R. Horst, P.M. Pardalos, Handbook of Global Optimization 2 Springer Science & Business Media, 2013.
- [21] Hurst, J., Rizzi, A., Hobbelen, D., 2004. Series elastic actuation: Potential and pitfalls. In: International Conference on Climbing and Walking Robots.
- [22] Jafari, A., 2014. Coupling between the output force and stiffness in different variable stiffness actuators. In: Actuators., vol. 3. Multidisciplinary Digital Publishing Institute, 270–284.
- [23] A. Jafari, N. Tsagarakis, D. Caldwell, Energy efficient actuators with adjustable stiffness: a review on awas, awas-ii and compact vsa changing stiffness based on lever mechanism, Ind. Robot.: Int. J. 42 (3) (2015) 242–251.
- [24] A. Jafari, N.G. Tsagarakis, D.G. Caldwell, Awas-ii: a new actuator with adjustable stiffness based on the novel principle of adaptable pivot point and variable lever ratio, Robot. Autom. (ICRA), 2011 IEEE Int. Conf. (2011) 4638–4643 (IEEE).
- [25] A. Jafari, N.G. Tsagarakis, D.G. Caldwell, Exploiting natural dynamics for energy minimization using an actuator with adjustable stiffness (awas), 2011 IEEE Int. Conf. Robot. Autom. (2011) 4632–4637 (IEEE).
- [26] A. Jafari, N.G. Tsagarakis, D.G. Caldwell, A novel intrinsically energy efficient actuator with adjustable stiffness (awas), IEEE/ASME Trans. Mechatron. 18 (1) (2011) 355–365.
- [27] A. Jafari, N.G. Tsagarakis, I. Sardellitti, D.G. Caldwell, How design can affect the energy required to regulate the stiffness in variable stiffness actuators, 2012 IEEE Int. Conf. Robot. Autom. (2012) 2792–2797 (IEEE).
- [28] A. Jafari, N.G. Tsagarakis, B. Vanderborght, D.G. Caldwell, A novel actuator with adjustable stiffness (awas), 2010 IEEE/RSJ Int. Conf. Intell. Robots Syst. (2010) 4201–4206 (IEEE).
- [29] A. Jafari, H.Q. Vu, F. lida, Determinants for stiffness adjustment mechanisms, J. Intell. Robot. Syst. 82 (3–4) (2016) 435–454.
- [30] Kim, W.S., Bejczy, A.K., Hannaford, B., 1991. Active compliance and damping in telemanipulator control.
- [31] C.A. Klein, R.L. Briggs, Use of active compliance in the control of legged vehicles, IEEE Trans. Syst., Man, Cybern. 10 (7) (1980) 393–400.
- [32] E.L. Lawler, D.E. Wood, Branch-and-bound methods: a survey, Oper. Res. 14 (4) (1966) 699–719.
- (1966) 699–719. [33] K.Y. Lee, M.A. El-Sharkawi, Modern Heuristic Optimization Techniques: Theory
- and Applications to Power Systems, John Wiley & Sons., 2008.
 [34] T. Ménard, G. Grioli, A. Bicchi, A stiffness estimator for agonistic-antagonistic
- variable-stiffness-actuator devices, IEEE Trans. Robot. 30 (5) (2014) 1269-1278. [35] Messine, F., Monturet, V., Nogarède, B., An interval branch and bound method
- dedicated to the optimal design of piezoelectric actuators, 2001.

 [36] F. Messine, B. Nogarede, J.-L. Lagouanelle, Optimal design of electromechanical
- actuators: a new method based on global optimization, IEEE Trans. Magn. 34 (1) (1998) 299–308.
- [37] R.E. Moore, R.B. Kearfott, M.J. Cloud, Introduction to Interval Analysis 110 Siam, 2009.
- [38] M. Okada, Y. Nakamura, S. Ban, Design of programmable passive compliance shoulder mechanism, Proc. 2001 Icra. IEEE Int. Conf. Robot. Autom. (Cat. No. 01CH37164) 1 (2001) 348–353 (IEEE).
- [39] N. Paine, S. Oh, L. Sentis, Design and control considerations for high-performance series elastic actuators, IEEE/ASME Trans. Mechatron. 19 (3) (2013) 1080–1091.
- [40] F. Petit, M. Chalon, W. Friedl, M. Grebenstein, A. Albu-Schäffer, G. Hirzinger, Bidirectional antagonistic variable stiffness actuation: Analysis, design & implementation, 2010 IEEE Int. Conf. Robot. Autom. (2010) 4189–4196 (IEEE).
- [41] Pratt, G.A., Williamson, M.M., Series elastic actuators. In: Proceedings 1995 IEEE/ RSJ International Conference on Intelligent Robots and Systems. Human Robot Interaction and Cooperative Robots, 1.IEEE, 399–406, 1995.
- [42] J. Pratt, B. Krupp, C. Morse, Series elastic actuators for high fidelity force control, Ind. Robot.: Int. J. 29 (3) (2002) 234–241.

- [43] H. Ratschek, J. Rokne, New Computer Methods for Global Optimization, Horwood. Chichester. 1988.
- [44] Robinson, D.W., Design and analysis of series elasticity in closed-loop actuator force control. Ph.D. thesis, Massachusetts Institute of Technology, 2001.
- [45] A. Schepelmann, K.A. Geberth, H. Geyer, Compact nonlinear springs with user defined torque-deflection profiles using cam mechanism for variable stiffness actuators, 2014 IEEE Int. Conf. Robot. Autom. (icra) (2014) 3411–3416 (IEEE).
- [46] R. Schiavi, G. Grioli, S. Sen, A. Bicchi, Vsa-ii: a novel prototype of variable stiffness actuator for safe and performing robots interacting with humans, 2008 IEEE Int. Conf. Robot. Autom. (2008) 2171–2176 (IEEE).
- [47] M. Solimanpur, A. Jafari, Optimal solution for the two-dimensional facility layout problem using a branch-and-bound algorithm, Comput. Ind. Eng. 55 (3) (2008) 606–619.
- [48] A. Solovyev, M.S. Baranowski, I. Briggs, C. Jacobsen, Z. Rakamarić, G. Gopalakrishnan, Rigorous estimation of floating-point round-off errors with symbolic taylor expansions, ACM Trans. Program. Lang. Syst. (TOPLAS) 41 (1) (2018) 1–39.
- [49] Stramigioli, S., van Oort, G., Dertien, E., A concept for a new energy efficient actuator.In: 2008 IEEE/ASME International Conference on Advanced Intelligent Mechatronics.IEEE, 671–675, 2008.
- [50] J. Sun, Z. Guo, D. Sun, S. He, X. Xiao, Design, modeling and control of a novel compact, energy-efficient, and rotational serial variable stiffness actuator (svsaii), Mech. Mach. Theory 130 (2018) 123–136.
- [51] J. Sun, Z. Guo, Y. Zhang, X. Xiao, J. Tan, A novel design of serial variable stiffness actuator based on an archimedean spiral relocation mechanism, IEEE/ASME Trans. Mechatron. 23 (5) (2018) 2121–2131.
- [52] Tonietti, G., Schiavi, R., Bicchi, A., Design and control of a variable stiffness actuator for safe and fast physical human/robot interaction.In: Robotics and Automation, 2005. ICRA 2005. Proceedings of the 2005 IEEE International Conference on.IEEE, 526–531, 2005.
- [53] N.G. Tsagarakis, I. Sardellitti, D.G. Caldwell, A new variable stiffness actuator (compact-vsa): design and modelling, 2011 IEEE/RSJ Int. Conf. Intell. Robots Syst. (2011) 378–383 (IEEE).
- [54] P.J. Van Laarhoven, E.H. Aarts, Simulated annealing, Simulated Annealing: Theory and Applications, Springer, 1987, pp. 7–15.
- [55] B. Vanderborght, A. Albu-Schäffer, A. Bicchi, E. Burdet, D. Caldwell, R. Carloni, M. Catalano, G. Ganesh, M. Garabini, M. Grebenstein, et al., Variable impedance actuators: moving the robots of tomorrow, 2012 IEEE/RSJ Int. Conf. Intell. Robots Syst. (2012) 5454–5455 (IEEE).
- [56] B. Vanderborght, A. Albu-Schäffer, A. Bicchi, E. Burdet, D.G. Caldwell, R. Carloni, M. Catalano, O. Eiberger, W. Friedl, G. Ganesh, et al., Variable impedance actuators: a review, Robot. Auton. Syst. 61 (12) (2013) 1601–1614.

- [57] B. Vanderborght, R. Van Ham, D. Lefeber, T.G. Sugar, K.W. Hollander, Comparison of mechanical design and energy consumption of adaptable, passive-compliant actuators, Int. J. Robot. Res. 28 (1) (2009) 90–103.
- [58] B. Vanderborght, B. Verrelst, R. Van Ham, M. Van Damme, D. Lefeber, B.M.Y. Duran, P. Beyl, Exploiting natural dynamics to reduce energy consumption by controlling the compliance of soft actuators, Int. J. Robot. Res. 25 (4) (2006) 343–358.
- [59] T. Verstraten, P. Beckerle, R. Furnémont, G. Mathijssen, B. Vanderborght, D. Lefeber, Series and parallel elastic actuation: Impact of natural dynamics on power and energy consumption, Mech. Mach. Theory 102 (2016) 232–246.
- [60] Visser, L.C., Carloni, R. , Stramigioli, S., Energy efficient control of robots with variable stiffness actuators.IFAC Proceedings Volumes 43 (14), 1199–1204, 2010.
- [61] Visser, L.C., Stramigioli, S., Bicchi, A., Embodying desired behavior in variable stiffness actuators.IFAC Proceedings Volumes 44 (1), 9733–9738, 2011.
- [62] Vwasriable impedance actuation systems embodying advanced interaction behaviORS 2014.ln:(https://viactors.org/).
- [63] W. Wang, R.N. Loh, E.Y. Gu, Passive compliance versus active compliance in robot-based automated assembly systems, Ind. Robot.: Int. J. 25 (1) (1998) 48–57.
- [64] S. Wolf, G. Grioli, O. Eiberger, W. Friedl, M. Grebenstein, H. Höppner, E. Burdet, D.G. Caldwell, R. Carloni, M.G. Catalano, et al., Variable stiffness actuators: Review on design and components, IEEE/ASME Trans. Mechatron. 21 (5) (2015) 2418–2430.

Trevor Exley: is a PhD student with the Department of Biomedical Engineering, at the University of North Texas.

Amir Jafari received the Ph.D. degree in robotics from the Italian Institute of Technology (IIT), Italy, in 2011. He is currently an associate professor with the Department of Biomedical Engineering, at the University of North Texas. Prior to this he was an assistant professor with the Department of Mechanical Engineering, at the University of Texas at San Antonio. From 2011 to 2012, he was a postdoctoral researcher with the IIT and from 2012 to 2013, he was a postdoctoral researcher with Swiss Federal Institute of Technology ETH in Zurich, Switzerland. From 2014 to 2016, he was with the Agency of Science, Technology and Research, Singapore, before he joined University of Texas at San Antiono UTSA in 2016. From 2016 to 2021 he was an assistant professor with the department of Mechanical Engineering at UTSA. Since September 2021, he is an associate professor with the department of Biomedical Engineering at the University of North Texas UNT.